2018 IEEE International Conference on Robotics and Automation (ICRA)
May 21-25, 2018, Brisbane, Australia

Landmark-based Exploration with Swarm of Resource Constrained Robots

Rattanachai Ramaithititima[1]

Subhrajit Bhattacharya[2]

***Abstract*— In this paper we consider the problem of autonomous exploration of an unknown, GPS-denied environment using a swarm of robots with very limited resources and limited sensing capabilities. To that end we use a *landmark complex,* a simplicial complex utilizing an observation of landmarks, as a topological representation of the environment. Each robot is equipped with an omni-directional, limited-range sensor that can identify landmarks in the robot's neighborhood. The robots use the bearing angles to the landmarks for local navigation. Given a collection of identifiable landmarks, a landmark complex can then be cumulatively constructed to encapsulate the topological information of the environment. Under the assumption of sufficiently dense landmarks, we propose an exploration and exploitation strategy that guides the swarm of robots to explore an environment using only bearing measurements without any metric information. Lastly, we demonstrate the coordinate-free and localization-free navigation in the environment using the constructed landmark complex.**

I. INTRODUCTION

A. Motivation and Related Work

In this paper we address the problem of *exploration* of an unknown, GPS-denied environment using a robot swarm with limited sensing capabilities, which we use to create a faithful topological representation of the environment. We then address the problem of *exploiting* this representation for metric-free and coordinate-free robot navigation in such a GPS-denied environment.

While simultaneous localization and mapping (SLAM) is not a new research area, most state-of-the-art methods require precise metric information (such as range measurements to obstacles), rely on relatively precise odometry measurements, and require extensive post-processing in order to correct for accumulated errors to build a complete map [1], [2], [3], [4], [5], [6]. Hence the representations of the environment that the robots build is not coordinate-free (e.g., an occupancy grid). The problem becomes even more complex when multiple robots need to build such a map simultaneously since the amount of information that needs to be shared between robots is extremely large and a precise transformation between the robots' local coordinates is difficult to compute [7], [8].

We, on the other hand, address the problem where multiple robots with only on-board limited-range sensors detect presence of landmarks within their respective sensing disks, but no distance measurements to the landmarks are available. Without knowing its own location, nor the locations of other robots in the environment (globally or relative to itself), the robots only communicate to other robots the identity of the landmarks that they see, which allows the robots to build the map collectively and in a distributed fashion. The method we propose is purely topological in nature which uses a simplicial complex as the representation of the environment. Specifically, we consider a *landmark complex,* a simplicial complex constructing by the observation of landmarks [9]. The landmark complex can capture the correct topology of the environment (i.e., is homotopy equivalence) under certain assumption on the density of landmarks. While even a rudimentary control strategy such as random walk is sufficient to build the map as long as the robots collectively see all the landmarks, we develop a more efficient control strategy for local robot navigation using coarse bearing measurements to the landmarks.

[1]University of Pennsylvania. ramar@seas.upenn.edu
[2] Lehigh University. sub216@lehigh.edu
We gratefully acknowledge the support of the Office of Naval Research (grant number N000141410510). We would also like to thank Dr. Vijay Kumar for his valuable discussions and suggestions on this work.

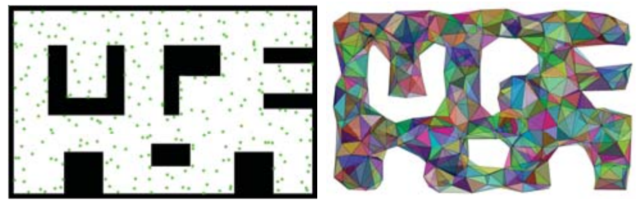

Fig. 1. **Overview:** Illustration of the geometric realization of the *landmark complex* (right) that represents the environment (left). The map is constructed from a collections of observations of the distinguishable landmarks (green stars) by the robots during exploration.

The strength of our algorithm lies in its simplicity of representation as a landmark complex, the ease in inter-robot communication of that representation, and hence the scalability to large robot swarms for cooperative construction of the map. While there has been extensive work in swarm robotics [10], the need for swarm algorithms to be scalable has been the bottleneck in addressing the exploration and mapping problems using large swarms. The focus of swarm literature has thus primarily been on solving problems such as coverage [11] and estimation [12], [13].

The choice of bearing-based controller is inspired by the literature on visual homing navigation [14], [15]. Our exploitation of the landmark complex for localization-free navigation also yields results similar to the visual memory exploitation technique appeared in [14].

B. Contribution

The main contributions of this work are the following. First, we establish the necessary and sufficient conditions that guarantee the completeness of our metric-free exploration. Second, we develop the landmark-based exploration algorithm that constructs a topological representation of an environment using swarms of robots with limited resources and capability. Lastly, we verify that the constructed landmark

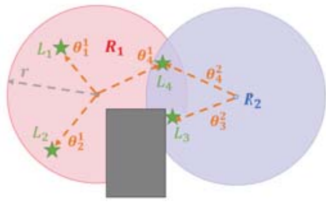

Fig. 2. **Sensing Model:** $S_1 = \{L_1, L_2, L_4\}$, and $S_2 = \{L_3, L_4\}$. The measurement for robot R_1 are $\theta_1^1, \theta_2^1, \theta_4^1$, , which be used to calculate relative bearing $\theta_{12}^1, \theta_{24}^1, \theta_{41}^1$. Although L_3 is within radius r from R_1, it is occluded by obstacle and hence not a member of S_1.

complex can be used for coordinate-free and localization-free navigation.

The paper is organized as follows. In the next section, we introduce the notation used in this paper, then provide the brief summary of the bearing-based controller and the frontier-based exploration strategy used in this work. In Section III, we provide the definition of landmark complex and then discuss the sufficient and necessary condition of the landmark distribution regarding landmark-based exploration. Section IV presents the full details of our algorithmic design. In Section V, we thoroughly evaluate the proposed method in simulation on various environments with team of up to 30 robots.

II. Preliminaries

A. Notations

We denote by $W \subset \mathbb{R}^2$ the obstacle free region where the swarm of robots can be deployed to explore the environment. Our objective is to deploy a swarm of N robots, denoted by $\{R_i\}_{i=1}^N$, to explore W and construct a sparse map that encapsulate all topological features of the environment. The position of R_i is denoted as $x_i \in W$, and we represent the set of the positions of all the robots as $X = \{x_1, x_2, ..., x_n\}$.

Given a collection of m identifiable, stationary landmarks, $\{L_i\}_{i=0}^m$, we represent the position of L_i as $y_i \in W$, and represent the set of the positions of all the landmarks as $Y = \{y_1, y_2, ..., y_m\}$. A robot, R_i, equipped with an omni-directional camera, can measure the bearing toward the landmarks within its disk-shaped sensing footprint of radius r. Thus, $S_i = \{L_j \mid \|x_i - y_j\| \leq r, \text{ and } \forall \alpha \in [0,1], (1-\alpha)x_i + \alpha y_j \in W\}$ denotes the set of landmarks detected by R_i. The bearing measurement (relative to a fixed reference direction) to landmark $L_j \in S_i$ is denoted by $\theta_j^i \in [-\pi, \pi)$. The relative bearing between landmarks $L_j, L_k \in S_i$ is defined as $\theta_{jk}^i = (\theta_k^i - \theta_j^i) \mod 2\pi$, which is between 0 and 2π. Given an observation S_i by robot R_i, let $\boldsymbol{\theta}_i = \{\theta_j^i | L_j \in S_i\}$ denotes the snapshot of bearing measurement by R_i. Figure 2 illustrates the sensing model of two robots with four landmarks. All landmarks are within the distance of r from R_1. However, $S_1 = \{L_1, L_2, L4\}$ because L_3 is occluded from the line-of-sight of R_1.

We assume a very simple obstacle detection model: A robot can detect and identify the general direction of an obstacle only upon contact.

B. Configuration and Bearing-based Controller

We assume that the robots are holonomic, hence the configuration of each robot is simply the position, $x \in W \subseteq \mathbb{R}^2$. Even when each robot has an orientation w.r.t a global frame, we assume that they can determine their own orientations either by using magnetometer or by sharing inter-robot bearing measurement. The robots are locally controlled using the bearing-only navigation system presented in [15]. By converting bearing angles to unit vectors in local coordinate, this controller utilizes the orthogonal components as a navigation vector field.

Given bearing angles, θ_a^i, θ_b^i, to landmarks L_a, L_b, let $\hat{\gamma} = [\cos(\theta_\gamma^i), \sin(\theta_\gamma^i)], \gamma = a, b$, denote a unit vector in their directions in local coordinates, and let $(\hat{a}^*, \hat{b}^*)$ denote the destination bearing unit vectors. The orthogonal vector of current bearing, $\hat{\gamma}^\perp$, is defined as

$$\hat{\gamma}^\perp = \begin{bmatrix} 0 & -1 \\ 1 & 0 \end{bmatrix} \hat{\gamma}$$

The control input is then defined as

$$u = -\sum_{\gamma \in \{a,b\}} \left(\hat{\gamma}^{*T} \hat{\gamma}^\perp\right) \hat{\gamma}^\perp.$$

This control policy is globally asymptotically stable [15], so the bearing measurement is guaranteed to converge to the destination. In a nutshell, this control law minimizes the projection of the orthogonal components of current bearing toward landmarks onto the destination ones. Hence, the vector representing current bearing will align with desired one when the orthogonal projection reaches zero.

C. Multi-robot Exploration

To demonstrate the application of landmark complex in exploration task, we adapt the frontier-based coordinated strategy from [16], which has an assumption of centralized coordination. The frontier assignment and the mapping occur in a centralized manner, while each robot executes their task individually. In summary, the exploration process can be divided into three general steps as the following.

1) Identify all unexplored frontiers.
2) Calculate the cost-utility function for each frontier for all robots.
3) Update the map as robots navigate to the frontiers

Generally, the cost-utility function is the estimated difference between profits (utility) and expenses (cost), which can be defined as the following.

Cost: The cost function is the distance between current location and the frontier.

Utility: The utility function is the expected information gain, which can be defined as the expected area that a robot will explore.

III. Landmark Complexes

In this section, we first provide a brief overview of algebraic topology and introduce the landmark complex. Then, we discuss the minimal density of the landmarks required for successful mapping and navigation using the notion of dispersion.

A. Algebraic Topology

A simplicial complex, informally speaking, is a higher dimensional generalization of a graph, which not only consists

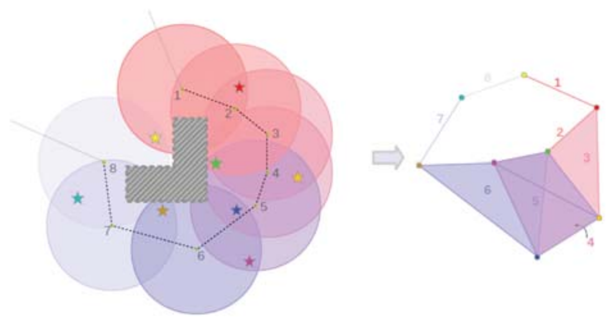

Fig. 3. **Landmark Complex** (right): Being constructed by a robot wandering in an environment (dashed trajectory) and observing the landmarks (colored stars), the landmark complex captures the topology of the workspace (left) correctly where a hole corresponds to an obstacle.

of 0-simplices (vertices) and 1-simplices (edges), but also their higher-dimensional counterparts such as 2-simplices, 3-simplices and so on. As a consequence, it is possible to create a topologically equivalent piece-wise linear representation of a configuration space of dimension 2 or more using a simplicial complex. We start with the formal combinatorial definition of a simplicial complex.

Definition 1 (Simplicial Complex [17])**.** A simplicial complex, $\mathcal{S}$, constructed over a set V (the *vertex set*) is a collection of sets $C_n,\ n = 0, 1, 2, \cdots$, such that

i. An element in $C_n,\ n \geq 0$ is a subset of V and has cardinality $n+1$ (*i.e.*, For all $\sigma \in C_n,\ \sigma \subseteq V, |\sigma| = n+1$). σ is called a "*n-simplex*" (*Simplex definition*).

ii. If $\sigma \in C_n,\ n \geq 1$, then $\sigma - v \in C_{n-1},\ \forall v \in \sigma$. Such a $(n-1)$-simplex, $\sigma - v$, is called a "*face*" of the simplex σ (*Boundary property*).

The simplical complex is the collection $\mathcal{S} = \{C_0, C_1, C_2, \cdots\}$.

In particular, we consider a simplicial representation of the environment called the *landmark complex* – a simplicial complex constructed from the observation of landmarks in the environment [9].

The construction of a landmark complex requires that the robots detect presence of distinguishable landmarks within their respective sensing footprints, but no distance or bearing measurements to the landmarks are necessary.

A *landmark complex*, $\mathcal{L} = \{C_0, C_1, C_2, \cdots\}$, is an abstract simplicial complex constructed over a set of distinct landmarks, $\{L_1, L_2, \cdots\}$, based on observations made by robots with limited-range sensors navigating in the environment, and is described as follows: Every time a robot observes a n-tuple of landmarks, it inserts the corresponding $(n-1)$-simplex in C_{n-1} (along with all its faces and subfaces in $C_i, i < n-1$), as illustrated in Figure 3.

Under certain density assumption on the landmarks and robot observations, a landmark complex is a truthful topological representation of the environment (homotopy equivalence). The landmark density requirement itself is that at least one landmark needs to be visible from every point in the environment. Or, in other words, the *visibility domains* of the landmarks (disks of same radius as the sensing radius, centered at each landmark), $\{\mathcal{V}_j\}$, need to cover the entire workspace of the robots. With this condition, and sufficiently dense sampling of observations by the robots, the landmark complex is identical to the *Cech complex* (or *nerve*) of the visibility domains of the landmarks (since every n-way overlap of the visibility domains, $\mathcal{V}_{i_1 i_2 \cdots i_n} = \mathcal{V}_{i_1} \cap \mathcal{V}_{i_2} \cap \cdots \cap \mathcal{V}_{i_n}$, corresponds to a potential observation of those n landmarks by a robot in $\mathcal{V}_{i_1 i_2 \cdots i_n}$), and hence by the *Nerve theorem*, homotopy equivalent to the workspace W.

Additionally, by Dowker's theorem [18], the dual of landmark complex, denoted by *observation complex* is an abstract simplicial complex, whose vertices are the set of observations, and an $n-$simplex represents the set of $n+1$ observations that share some landmarks in common. We will use this property later in the exploitation strategy.

B. Dispersion

We borrow the notion of *dispersion* from sampling theory [19] to numerically quantify the sparsity of landmark distribution. The dispersion of a finite set P of samples in a metric space $(\mathcal{X}, \rho)$ is

$$\delta(P) = \sup_{x \in \mathcal{X}} \{\min_{p \in P} \{\rho(x, p)\}\}$$

Using L_2 metric, the L_2 dispersion in $\mathbb{R}^2$ can viewed as the radius of the largest ball that does not touch any sample points p.

The dispersion of the landmarks $\delta(\{L_i\})$ or simply δ over L_2 metric is defined as

$$\delta = \sup_{x \in W} \{\min_{y_j \in Y} \{\|x - y_j\|\}\}$$

Hence, the upper bound of the dispersion is r so that every point in the environment can observe at least one landmark.

Nevertheless, observing one landmark is insufficient for bearing-based navigation. Each robot requires at least two landmarks assuming that the orientation is fixed.

IV. Algorithmic Design

The outline of our swarm exploration algorithm is presented in Algorithm 1. The exploration process occurs in an iterative manner until all frontiers are explored. In line 2, the process begins with identifying the set of frontiers – a collection of unexplored areas as defined in Section IV-A. As the robots *explore* beyond the frontiers, they construct the landmark complex $\mathcal{L}$, and thus *exploit* it for navigation by constructing its dual navigation graph $\mathcal{G}$ in line 3. Since landmark complex is a topological representation of the entire environment, it is constructed cumulatively (see Algorithm 2), while the navigation graph $\mathcal{G}$ is computed for each instance of $\mathcal{L}$ as described in Section IV-B.

Using the navigation graph $\mathcal{G}$ and the list of frontiers $\mathcal{F}$, we compute the cost-utility for all pairs of free robots R_i and frontiers $\langle a, b\rangle \in \mathcal{F}$ in line 5. We then choose the pair of the frontier $\langle a, b\rangle$ and free robot R_i such that the cost-utility function is maximized in line 6. The assignment table, A, is used to keep track of the current assignment, where $A[i] = \{a, b\}$ denotes frontier $\langle a, b\rangle$ is assigned to R_i.

The robot-to-frontier assignment can be done using the greedy algorithm for simplicity or the Hungarian algorithm for the optimal assignment. However, since the task assigned to one robot affects the utility function of other robots, it is not trivial to apply the Hungarian algorithm. Furthermore, although all robots begin as free, each robot will execute its assigned task in parallel and may not finish at the same time. The task assignment will often occur in asynchronous manner and thus the benefit of Hungarian algorithm would be diminished.

After receiving an assignment, each robot individually navigates to its assigned frontier using the bearing-based controller and the navigation graph $\mathcal{G}$. As the swarms navigate and explore the environment, their observations are used for cumulatively updating the landmark complex $\mathcal{L}$ and frontier list $\mathcal{F}$.

Algorithm 1 Swarm Exploration Overview

```
do
    Identify the set of frontiers F
    Construct/update the landmark complex L and compute the navigation graph G.
    while exist robot with no frontier assignment do
        Compute the cost-utility for each free robot R_i with each frontier ⟨a, b⟩ ∈ F.
        Assign frontier to free robot with maximal cost-utility function .
    end while
while F ≠ ∅
```

A. *Frontier Identification*

In frontier-based exploration, the boundaries of the unexplored regions constitute frontiers. In our case, a frontier constitutes of an ordered pair of landmarks with the order describing the orientation of the frontier region.

With m landmarks, there are $m(m-1)$ combinations of possible frontiers. At the beginning, all frontiers' statuses are unknown. As robots explore the environment, the frontiers are identified using relative bearing measurements. Given an observation S_i, every pair of landmarks and orientations become potential frontiers. The potential frontier is then either identified as *clear* or *unexplored*. Once the frontier is marked as clear, it will remain unchanged throughout the exploration. The objective of the exploration process is then to clear all unexplored frontiers.

A frontier can be cleared in two ways. Firstly, the frontier is observed as part of the inner diagonal of the explored polygon, where an explored polygon is the convex hull of the observed landmarks. Without the range measurement to landmarks, we use the relative bearing to determine whether the observation occur inside or outside the explored polygon. The largest relative bearing between any two adjacent landmarks can be larger than π if and only if the observation occurs outside the explored polygon. This is checked by sorting the bearing in the polar coordinate system and calculating the different between the adjacent landmarks on the list. Figure 4 illustrates the examples of observation that occurs inside and outside the explored polygon during exploration process. With limited information, either half of the potential frontiers are cleared or all of them are marked as unexplored for each observation.

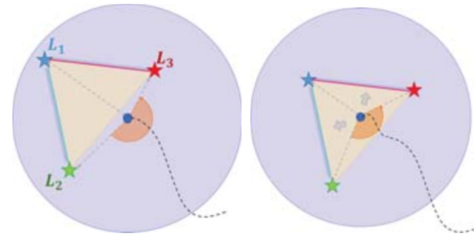

Fig. 4. **Frontier Identification:** A method to determine the frontiers during exploration process. The robot is assigned to explore frontier $\langle 2,3\rangle$ with the current observation includes three landmarks $\{L_1, L_2, L_3\}$. The explored polygon is shaded in yellow and the largest relative bearing is shaded in orange. Before getting inside the explored polygon (left), the largest relative bearing is larger than π and none of the frontiers is cleared. After moving inside the explored polygon (right), the bearing becomes smaller than π and three of the potential frontiers, including the assigned frontier, $\langle 1,2\rangle$, $\langle 2,3\rangle$, $\langle 3,1\rangle$ are cleared.

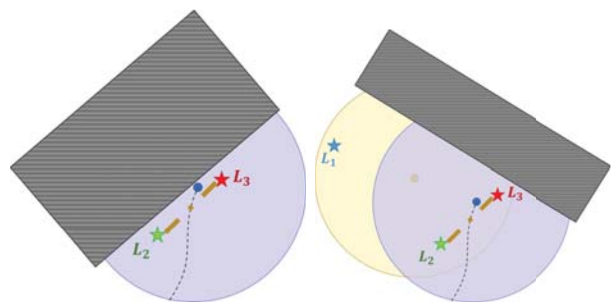

Fig. 5. **Obstacle Boundary:** A frontier constituting of the boundary of the obstacle. In the first case (left), the robot hit the obstacle right after crossing the edge and cannot continue the exploring $\langle 2,3\rangle$, so $\langle 2,3\rangle$ can be masked as obstacle boundary. On the other hand (right), the robot can continue exploration for a while after crossing the boundary into $\langle 2,3\rangle$. Thus, the status of $\langle 2,3\rangle$ is uncertain. Although $\langle 2,3\rangle$ is not an obstacle boundary, the desired observation occurs at the position denoted by the yellow striped disk, where the robot may or may not reach.

Secondly, the frontier is cleared if it is an obstacle boundary, i.e., a boundary that is adjacent to the obstacles. For actual obstacle boundary, the robot will most likely run into obstacles which can then be detected. On the other hand, it is difficult to determine that the frontier is not the boundary without any filtering process as illustrated by Figure 5. There are two potential solutions to resolve this.

The first solution involves tracing the $1-$skeleton of the landmark complex after the exploration is completed. By setting a time limit for each robot to randomly explore the frontier, the frontier, that is undetermined after timeout, is marked as potential obstacle boundary. After the exploration process is completed, we calculate the $1-$skeleton of the landmark complex to trace of all obstacle boundaries and re-explored the potential boundaries that are inconsistent, i.e. there is an inconsistency between the obstacle boundary from the landmark complex and the actual boundary marked by the exploration process. Nevertheless, this approach does not guarantee any completeness as the frontier exploration relies on the random walk process.

On the other hand, we can decrease the unpredictability of the random walk during frontier exploration by decreasing the dispersion of the landmarks, i.e., making them denser. As dispersion decreases, the landmark becomes closer causing the overlapped regions to be larger. Hence, the robot is more

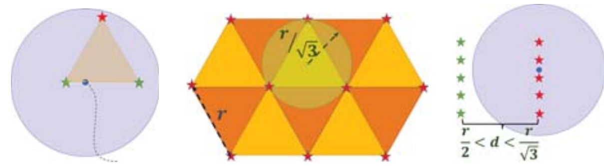

(a) Ideal Case (b) Triangular Tessellation (c) Bad Case

Fig. 6. **Landmark Distribution:** In ideal scenario, a robot can see other adjacent landmarks from any point along the boundary frontier. A robot can detect red landmark from any point along between two green landmarks. The optimal landmark distribution forms a triangular tessellation with side length of r and the circumscribed of equilateral triangle is $\frac{r}{\sqrt{3}}$. In bad distribution, the robot cannot detect other landmarks from the boundary even if $\delta \leq \frac{r}{\sqrt{3}}$.

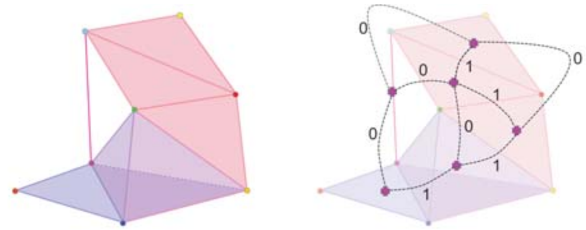

Fig. 7. **Navigation Graph (right):** The partial $1-$skeleton of *Observation complex*, a dual complex of landmark complex (left). A vertex on navigation graph corresponds to the free simplex in the observation complex, while an edge between them corresponds to two set of observations that shares common landmarks. The number on the edges represents the dimension of sub-simplex which is the number of common landmarks subtract by one.

likely to observe the simplices.

Ideally, the entire configuration along the edge between two landmarks should be contained inside the overlapped region so that crossing the boundary would suffice to clear the frontier as illustrated in Fig 6(a). In other words, the landmark complex constructed from observations of every boundary would suffice to capture all topological features of the environment. We consider the optimal and worst case to determine the upper and lower bound of δ.

Proposition 1. *The density of landmarks,* $\delta, \in [\frac{r}{2} \frac{r}{\sqrt{3}}]$ *is necessary and sufficient.*

The optimal landmark distribution occurs when all landmarks have the distance of r from each other. This forms a uniform triangular tessellation where each equilateral triangle has the side length of r (Fig 6(b)). Hence, the radius of the circumscribed of equilateral triangle provide the upper bound of the dispersion, $\delta \leq \frac{r}{\sqrt{3}}$. Nevertheless, it is not sufficient as one of the counter example illustrated in Figure 6(c).

For sufficient condition, we consider the worst case scenario when the landmarks form the lines with the maximal separation as illustrate in the counter example in Figure 6(c). Hence, without minimal distance between landmarks, the sufficient condition needs to constrain the separation between lines to r. As a result, the lower bound of the dispersion is $\frac{r}{2} \leq \delta$.

In practice, the necessary condition would be good enough since intersected regions is large enough that the robot will hardly miss it. Additionally, with the dispersion of $\frac{r}{\sqrt{3}}$, it will satisfy the necessary landmarks required for navigation in all scenarios as the landmarks become approximately three times denser. Note that additional landmarks may be required near the obstacle to satisfy the necessary condition for navigation.

B. Landmark Complex and Navigation Graph Construction

The landmark complex $\mathcal{L}$ is cumulatively constructed as the robots explore an environment. The update function is defined in Algorithm 2. For any given observation, the landmark complex is updated by adding simplices constructed from all possible combination of detected landmarks as defined in line 4. $\mathbb{P}(S_i)$ denotes the power set of S_i. Additionally, a bearing lookup table, BLT, is bookkeeping a snapshot of observed bearing for guidance during navigation. The landmark complex only need to be updated when changes occur in the set of detected landmarks and each robot may choose any instance of bearing measurement as the reference stored in BLT. Due to noisy measurement, one may use the average of multiple measurements to reduce the noise.

Algorithm 2 $[\mathcal{L}, BLT]$ = UPDATELC$(S_i, \boldsymbol{\theta}_i)$
Input: List of landmarks S_i and the bearing measurement $\boldsymbol{\theta}_i$.
Output: Landmark complex $\mathcal{L}$ and bearing lookup table BLT.

```
1: if L and BLT not initialize then
2:     L ← ∅, BLT = []
3: end if
4: L ← L ∪ (P(S_i) \ ∅)
5: BLT[S_i] = θ_i
```

We then construct the navigation graph $\mathcal{G} = (V_\mathcal{G}, E_\mathcal{G})$ which is a $1-$skeleton of the observation complex for exploiting the landmark complex. This graph can be viewed as a road map where each vertex represents a unique observation. To minimize the size of navigation graph, the vertex set $V_\mathcal{G}$ only consists of the *interesting* observations. An observation is interesting if it contains the unique combination of landmarks that cannot be observed elsewhere. We denote an interesting observation as *free simplex* in the landmark complex. The free simplex is a simplex that is not the face (or simply subset) of any other simplex.

$$V_\mathcal{G} = \{S_i \in \mathcal{L} |\ \forall S_j \in \mathcal{L} \setminus \{S_i\}, S_i \cap S_j \neq S_i\}$$

The edges are added for every pair of free simplices that share sufficient dimension of sub-simplex, n_l, required for navigation.

$$E_\mathcal{G} = \{(S_i, S_j) |\ S_i, S_j \in V_\mathcal{G}, S_i \neq S_j, |S_i \cap S_j| \geq n_l\},$$

where $n_l = 2$ for our holonomic robots.

Since we are only interested in the free simplices when constructing a navigation graph, it is sufficient to add only the simplex representing current observation to the landmark complex in line 4 of Algorithm 2.

C. Cost-Utility Function

The cost function $C(S_i, \langle a, b \rangle)$ is defined as the minimum distance from a vertex representing the current configuration, S_i, to one of the vertices adjacent to the frontier, $\{S_j \in V_\mathcal{G} |\ \{L_a, L_b\} \subseteq S_j\}$. Since there is no actual metric information that can measure the real distance needed to traverse an edge, we choose the dimension of overlapping sub-simplex to estimate the difficulty of traversing it, i.e. the number of common landmarks between two observations subtract by one. Hence, the weight can be defined as:

$$\forall (S_i, S_j) \in E_{\mathcal{G}}, W(S_i, S_j) = \frac{1}{|S_i \cap S_j| - 1}.$$

Given the weighted graph, the cost function can then be calculated using any graph-based searching method such as Dijkstra's or A*. The output of the graph-based searching method is cost to reach each frontier and the best sequences of observations that can guide the robot there.

The utility function $U(\langle a, b\rangle)$ is defined as the potential information gain from exploring that frontier. One potential indicator is the number of unexplored frontiers that share common landmarks with it. Additionally, the robot should avoid exploring the frontier in the same area as other robots. Hence, we define the utility function as:

$$U(\langle a, b\rangle) = \frac{|\{\langle c, d\rangle \in \mathcal{F} |\ \{L_a, L_b\} \cap \{L_c, L_d\} \neq \emptyset\}|}{|\{R_i |\ A[i] \cap \{a, b\} \neq \emptyset\}|}$$

Hence, the cost-utility function is defined as

$$CU(S_i, \langle a, b\rangle) = U(\langle a, b\rangle) - \beta \cdot C(S_i, \langle a, b\rangle),$$

where $\beta \geq 0$ determines the relative importance between utility and cost function.

D. Task Execution

The task assignment outputs the target frontier $\langle a, b\rangle$ and the sequence of observations, $S_{i_0}, S_{i_1}, ..., S_{i_k}$, that guides a robot to the assigned frontier, where S_{i_0} corresponds to the current observation and S_{i_k} corresponds to the observation adjacent to the assigned frontier. The execution consists of two phases: navigating to S_{i_k} and then explore $\langle a, b\rangle$.

In phase one, the robot uses bearing-based controller to go through the sequence of observations where the desired bearing is recorded in the lookup table BLT. Note that the sequence of observations is simply the guidance. For each target observation S_{i_j}, the robot does not require to reach the exact observation. It can skip to the next target as soon as it observes enough landmarks to reach the next one. Once the robot reaches a configuration where it can observe both landmarks L_a, L_b, it continues to the next phase.

In phase two, the robot begins by approaching the regions that constitute the frontier, i.e. driving toward areas between two corresponding landmarks if it is on the opposite side. After arriving at the right region, the robot begins exploring the frontier by searching for other landmarks that can be observed from this region. This can be done using biased random walk to search for locally. Each robot carries out phase two until either the frontier is identified or time limit is reached, where time limit depends on the dispersion of the landmarks.

V. Results

We demonstrate the performance of the landmark-based exploration through simulations on various setups using MATLAB. Then we show that the landmark complex constructed by the proposed method can be used for navigating

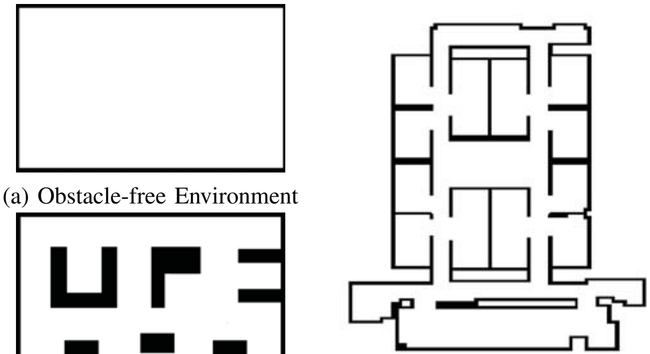

(a) Obstacle-free Environment

(b) Simple Environment

(c) Complex Environment

Fig. 8. **Testing Environments:** The topological exploration are evaluated on three different environments with teams of up to 30 robots.

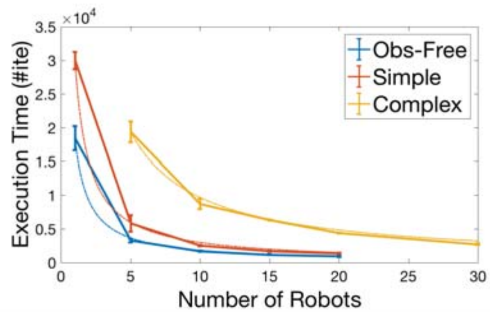

Fig. 9. **Execution Time vs. Number of Robots: The dashed-lines represent the expected completion time which is calculated by dividing the total execution time of the smallest team by the number of robots.**

a robot to a vertex in the observation complex. Lastly, we study the success rate of exploration with respect to δ.

In all studies, the bearing measurement has the Gaussian noise $\mathcal{N}(0, \sigma)$ with $\sigma = \frac{\pi}{72}$, which means that the errors are within 5 degrees 95% of the time.

A. Exploration

We evaluate our proposed method on three different environments: obstacle-free, simple structure, and complex structure, based on two criteria: completion rate and execution time. The landmarks are randomly generated with $\delta = \frac{r}{\sqrt{3}}$, averaging in 130, 260, and 800 landmarks, respectively.

The completion rate is measured as the percentage of the coverage area corresponding to the simplices that have been observed, while the execution time is measured by the number of iterations, where each iteration represents one movement and one measurement for each robot.

The completion rates are consistent across the number of robots with an average of 98% on an obstacle-free environment, 95% on a simple structure, and 91.5% on a complex structure. On the other hand, the execution times signify the efficiency of exploration with team of robots as illustrated in Figure 9. The outcomes beat the expectation in most cases, where the expected time is calculated by dividing the total execution time of the smallest team by the number of robots. Nevertheless, the efficiency rate slightly drops as the number of robots increases which could have resulted from limited space or poor coordination between robots.

(a) Coverage Map

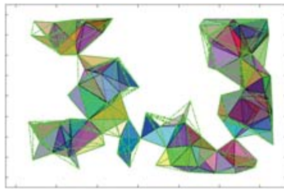

(b) Ite: 100

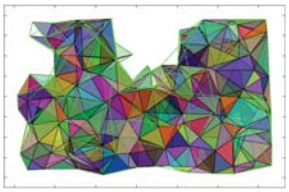

(c) Ite: 800

(d) Ite: 1864 (Final)

Fig. 10. **Obstacle-Free Environment:** Our algorithm finishes exploring the trivial environment filled with 133 landmarks using teams of 10 robots in 1864 iterations. Figure (a) illustrates the coverage map of all landmarks. Figures (b-d) show the geometric realization of the constructed landmark complex at different iteration, where green-dashed lines denote the unexplored frontiers. At the beginning, the landmark complex belongs to different homotopy class as it contains many connected components and holes. The disconnected components are linked and the holes are mended as more simplices are observed.

(a) Coverage Map

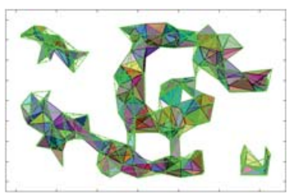

(b) Ite: 100

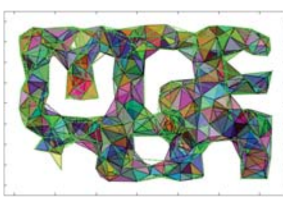

(c) Ite: 500

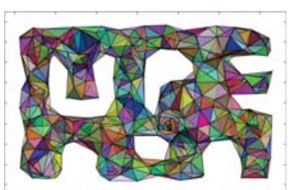

(d) Ite: 1266 (Final)

Fig. 11. **Simple structure:** The constructed landmark complex successfully captures all topological features of the environment with non-trivial topology, i.e. the number of holes is equal to the number of obstacles. The exploration with teams of 20 robots is completed in 1266 iterations.

Figure 10,11, and 12 illustrate the snapshots of geometric realization of the landmark complex constructed during exploration on all three environments. The geometric realization uses the approximated position of landmarks for the purpose of visualization only. The first top-left of each figure illustrates the coverage map of the landmarks, following by the updated landmark complex at various iterations. The coverage map is generated by overlaying the sensing disk from each landmark with different color. The progress are smaller and smaller toward the end as robots need to traverse larger distance to explores different frontiers including the *false* ones, which do not contribute any new information.

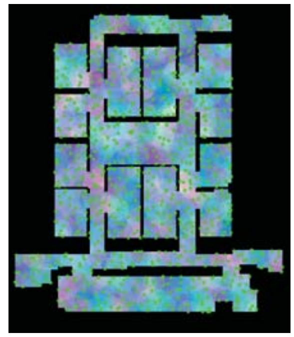

(a) Coverage Map

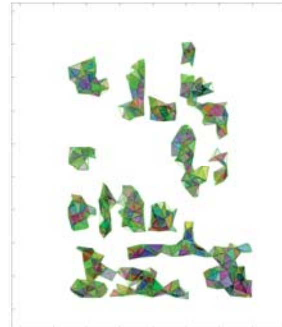

(b) Ite: 100

(c) Ite: 1000

(d) Ite: 2373 (Final)

Fig. 12. **Complex Environment:** The proposed method is evaluated on the large map resembling the building floor plan filled with 869 landmarks using team of 30 robots. The exploration is completed in 2373 iterations.

B. Exploitation

In this simulation, we demonstrate the exploitation of observation complex constructed by other robots in the past. The target are given as the set of observation and we use the navigation graph to guide the robot there.

C. Dispersion Analysis and Comparison

We demonstrates that our proposed method will succeed even in the worst case scenario if the landmarks are sufficiently dense. Since our proposed method consists of the random element in the second phase of execution (exploring the frontiers), we simulate the worst case scenario by minimizing the effort during the exploration phase.

In this experiment, we simulate the exploration with minimal effort on a small simple environment with $\delta = \{\frac{r}{2}, \frac{r}{\sqrt{3}}, \frac{r}{\sqrt{2}}, r\}$. The result is illustrated by the box plots in Figure 14.

The minimal effort exploration achieves an average completion rate of $0.984, 0.882, 0.803$, and 0.522 for $\delta = \{\frac{r}{2}, \frac{r}{\sqrt{3}}, \frac{r}{\sqrt{2}}, r\}$ respectively. This conforms with our assumption of sufficient and necessary condition for dispersion. For the execution time, the exploration process takes longer for the smaller dispersion since there are more landmarks and hence more frontiers to explore.

Lastly, we compare our proposed method with random walk exploration. Note that we use different criteria for termination of the exploration since there are some frontiers that are hard to be arbitrarily observed, resulting in high execution time of random walk process. For the sake of comparison, we use the completion rate of 95% , which

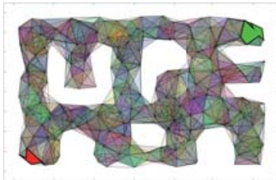

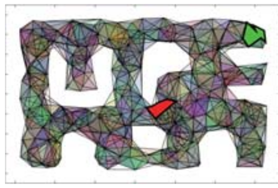

(a) Current (red) and Destination (green) observation

(b) Ite: 200

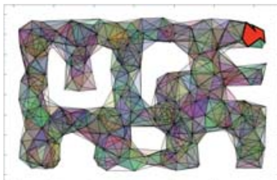

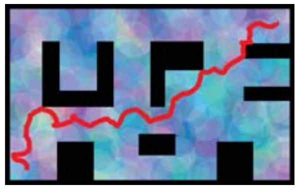

(c) Ite: 494 (Final)

(d) Paths taken by robot

Fig. 13. **Navigation Example:** Robot exploits the observation complex constructed by other robots for navigation from initial simplex to goal simplex.

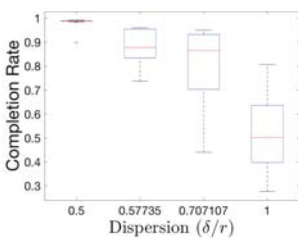

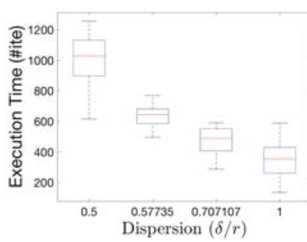

(a) Completion Rate

(b) Execution Time

Fig. 14. **Comparison on dispersion:** The box plots illustrate the completion rate and execution time of the proposed method with minimal effort during the frontier exploration. At the high dispersion, the landmarks are too sparse and hard to be observed, resulting in low completion rate when minimizing the efforts in frontier exploration. On the other hand, denser landmarks yields better coverage and hence gives higher completion rate with the trade-off of longer execution time due to significantly higher number of frontiers.

is unobservable in practice, as a stopping condition. Our proposed method performs about 3 times better than random walk in the small simple environment.

VI. Discussions

In this paper, we propose the metric-free exploration algorithm for the swarms of limited resources and sensing capabilities using a topological representation of an environment. Each robot is equipped with an omni-directional, limited range sensor that can identify landmarks in its neighborhood and measure their bearing angles for local navigation. The landmark complex, a simplicial complex that encapsulates the topological information of the environment, is constructed based on the observation of identifiable landmarks. With sufficiently dense landmarks, we demonstrate the performance of our proposed method on three environments with different structures in simulations. Additionally, the constructed landmark complex can be further exploited for future navigation.

Although our coordinate strategies are implemented in a centralized manner in this work, similar results can be achieved in a decentralized implementation if all robots can maintain a communication link with each other. Since the map representation is sparse and compact, the communication bandwidth is not be an issue. Of course, resource-constrained robots will also have limited range radios and may not be able to form a connected graph. This motivates the study of decentralized exploration algorithms and creating the landmark complex, an area of current investigation which we hope to report in future work.

References

[1] J. A. Castellanos, J. Montiel, J. Neira, and J. D. Tardós, "The spmap: A probabilistic framework for simultaneous localization and map building," *IEEE Transactions on Robotics and Automation*, vol. 15, no. 5, pp. 948–952, 1999.

[2] H. Choset and K. Nagatani, "Topological simultaneous localization and mapping (slam): toward exact localization without explicit localization," *IEEE Transactions on robotics and automation*, vol. 17, no. 2, pp. 125–137, 2001.

[3] M. Montemerlo, S. Thrun, D. Koller, B. Wegbreit, *et al.*, "Fastslam: A factored solution to the simultaneous localization and mapping problem," in *Proceedings of the AAAI National Conference on Artificial Intelligence*, pp. 593–598, 2002.

[4] H. Durrant-Whyte and T. Bailey, "Simultaneous localization and mapping: part i," *IEEE robotics & automation magazine*, vol. 13, no. 2, pp. 99–110, 2006.

[5] A. J. Davison, I. D. Reid, N. D. Molton, and O. Stasse, "Monoslam: Real-time single camera slam," *IEEE transactions on pattern analysis and machine intelligence*, vol. 29, no. 6, pp. 1052–1067, 2007.

[6] A. Angeli, D. Filliat, S. Doncieux, and J.-A. Meyer, "Fast and incremental method for loop-closure detection using bags of visual words," *IEEE Transactions on Robotics*, vol. 24, no. 5, pp. 1027–1037, 2008.

[7] S. Thrun and Y. Liu, "Multi-robot slam with sparse extended information filers," *Robotics Research*, pp. 254–266, 2005.

[8] A. Howard, "Multi-robot simultaneous localization and mapping using particle filters," *The International Journal of Robotics Research*, vol. 25, no. 12, pp. 1243–1256, 2006.

[9] R. Ghrist, D. Lipsky, J. Derenick, and A. Speranzon, "Topological landmark-based navigation and mapping," *University of Pennsylvania, Department of Mathematics, Tech. Rep*, vol. 8, 2012.

[10] N. Correll and H. Hamann, "Probabilistic modeling of swarming systems," in *Springer Handbook of Computational Intelligence*, pp. 1423–1432, Springer, 2015.

[11] K. Elamvazhuthi and S. Berman, "Optimal control of stochastic coverage strategies for robotic swarms," in *Proceedings of the IEEE International Conference on Robotics and Automation,*, pp. 1822–1829, IEEE, 2015.

[12] K. Elamvazhuthi, C. Adams, and S. Berman, "Coverage and field estimation on bounded domains by diffusive swarms," in *of the IEEE Conference on Decision and Control*, pp. 2867–2874, IEEE, 2016.

[13] Z. Lu, T. Ji, W. Tang, and Q. Wu, "Optimal harmonic estimation using a particle swarm optimizer," *IEEE Transactions on Power Delivery*, vol. 23, no. 2, pp. 1166–1174, 2008.

[14] A. A. Argyros, K. E. Bekris, S. C. Orphanoudakis, and L. E. Kavraki, "Robot homing by exploiting panoramic vision," *Autonomous Robots*, vol. 19, no. 1, pp. 7–25, 2005.

[15] S. G. Loizou and V. Kumar, "Biologically inspired bearing-only navigation and tracking," in *Proceedings of the IEEE Conference on Decision and Control*, pp. 1386–1391, IEEE, 2007.

[16] W. Burgard, M. Moors, C. Stachniss, and F. E. Schneider, "Coordinated multi-robot exploration," *IEEE Transactions on robotics*, vol. 21, no. 3, pp. 376–386, 2005.

[17] A. Hatcher, *Algebraic Topology*. Algebraic Topology, Cambridge University Press, 2002.

[18] C. H. Dowker, "Homology groups of relations," *Annals of mathematics*, pp. 84–95, 1952.

[19] S. M. LaValle, *Planning algorithms*. Cambridge university press, 2006.